On the Performance Comparison of UWB Waveforms for Fast Acquisition and Ranging in an Underground Mining Environment

Yassine SALIH ALJ[1,2], *Student Member, IEEE,* Charles DESPINS[1,2,3], *Senior Member, IEEE,*and Sofiène AFFES[1,2], *Senior Member, IEEE*

1: INRS-E.M. & Telecommunications, 800, De La Gauchetière West, Suite 6900, Montreal (QC) H5A 1K6 Canada.
2: Underground Communications Research Laboratory (LRCS), 450, 3d Av., Local 103, Val-d'Or (QC) J9P 1S2 Canada.
3: Prompt, 1155, University Street, Suite 903, Montreal (Qc) H3B 3A7 Canada.
Email: yassine@emt.inrs.ca; cdespins@promptinc.org; affes@emt.inrs.ca

Abstract **–** Ultra-wideband (UWB) communication systems provide very high data rates by transmitting extremely short duration pulses. The impulse waveform is one of the key factors that influence the performance of these systems. While fulfilling the FCC spectral emission requirements, the pulse shape must offer high detection capabilities with suitable levels of accuracy. In this paper, various pulse shapes are considered within a computationally-efficient fast acquisition system under different scenarios of interference and Gaussian noise in extensive Monte-Carlo simulations. The results show the 4th order Gaussian derivative as the most suitable pulse shape for this new UWB fast acquisition system suggested for ranging in a peculiar confined environment, which offers very acceptable positioning error range at high levels of noise and interference, while also yielding greatly reduced complexity and acquisition time.

I. INTRODUCTION

Ultra-wideband (UWB) radio is a fast emerging technology, currently regarded as an attractive solution for many wireless communication applications. As a carrier-free (baseband) wireless transmission technology, UWB radio utilizes ultra-short waveforms that are compatible with the FCC spectral masks. The resulting transmitted UWB signal is spread with a very low Power Spectral Density (PSD) over an absolute bandwidth of at least 500 MHz into a large spectrum (3.1-10.6 GHz) [1]. In addition to the PSD of the transmitted signal which is influenced by the used pulse shape, the performance of the UWB system itself may also be affected under non-ideal conditions [2]. Thus, the choice of the fundamental pulse shape used to generate an UWB signal is one of the most important considerations for an UWB system. In [3], the first ten Gaussian derivatives were compared in terms of their PSD and compliance to the FCC spectral constraints. For these pulses, higher-order derivatives have shown better fitting to the FCC masks with decreasing bandwidths as the order of the derivation increases. Indeed, as the pulse order increases, the number of zero crossings in the same pulse width also increases; the pulses begin to resemble sinusoids modulated by a Gaussian pulse-shaped envelope, thus corresponding to a higher "carrier" frequency sinusoid modulated by an equivalent Gaussian envelope [2]. Moreover, Gaussian-based pulse shapes outperform generally other UWB typical pulse types, as recently proposed in [4], and are noticeably easier to generate [5]. These observations lead to considering Gaussian-based, typically high-order derivatives, as the most potential candidates for UWB systems.

In this paper, we evaluate the impact of different Gaussian-based pulses on an UWB computationally-efficient fast acquisition system suggested for ranging within a peculiar multipath fading channel. Considerable research effort has been devoted recently to accelerate the timing acquisition in UWB systems. Based on different algorithmic approaches, several fast acquisition techniques, where the complexity aspect was generally less emphasized than the algorithmic one, were proposed [6-7]. In order to achieve a low-complexity receiver, an UWB computationally-efficient acquisition system showing explicit design characteristics that offer greatly improved computational cost and acquisition time was proposed in [8]. For this new UWB scheme based on a *Block-Processing* technique adapted to a FFT-based circular correlation, the pulse shape remains an important design factor to study in this paper. The performance levels of the first eleven Gaussian derivatives and the popular doublet waveform are compared in this paper to determine the most suitable pulse shapes to implement in the design of this typical fast acquisition scheme suggested for ranging over a peculiar indoor environment.

The remainder of this paper is organized as follows. In Section II, the used system concept is described and the characteristics of the Gaussian-based impulses are briefly highlighted. The considered UWB fast acquisition system is detailed in Section III. Section IV presents numerical results, and finally, Section V concludes the paper.

II. SYSTEM MODEL

In this section, we will describe the system model of the considered UWB communication system.

A. UWB Transmitter

Direct-Sequence (DS) UWB concept is employed in this paper with BPSK pulse signaling. The pulse occupies the entire chip interval and is transmitted continuously according to a MLS spreading code. The DS-UWB signal transmitted by a user k can typically be expressed as

$$s_{tr}^{(k)}(t) = \sum_{j=-\infty}^{j=+\infty} \sum_{n=0}^{N_c-1} d_j^{(k)} \cdot c_n^{(k)} \cdot p_{tr}(t - jT_f - nT_c), \qquad (1)$$

where $p_{tr}(t)$ represents the transmitted pulse shape (*i.e.* Gaussian 3rd-order derivative), $\{d_j\}$ represent the modulated data symbols mapped into $\{-1, 1\}$, $\{c_n\}$ are the spreading chips generated according to a MLS code, T_c is the chip duration. There are N_c chips per each message symbol j of period T_f − the spreading factor − such that $N_c . T_c = T_f$.

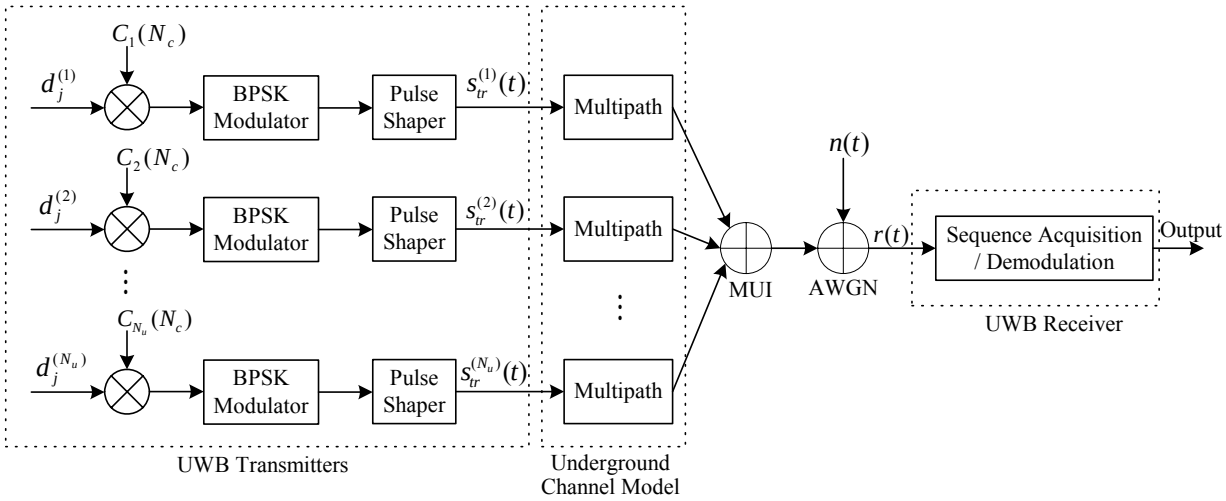

Fig.1: Block diagram of the considered system model.

B. Pulse Shape

The transmitted pulse shape used within an UWB system influences its spectral properties. The considered ultra-short pulse duration T_c is 2 ns, so the effective UWB signal bandwidth is at least 500 MHz. Moreover, due to antenna effects, the processed pulse at the receiver is modeled as a derivative of the transmitted pulse shape. The basic Gaussian pulse is expressed as

$$p(t) = \frac{1}{\sqrt{2\pi\sigma}} \exp(-\frac{t^2}{2\sigma^2}), \tag{2}$$

where σ is a shape factor used typically as a bandwidth decaying parameter. The nth order Gaussian derivative can be determined recursively from

$$p_n(t) = -\frac{n-1}{\sigma^2} p_{n-2}(t) - \frac{t}{\sigma^2} p_{n-1}(t) \cdot \tag{3}$$

The amplitude spectrum of the nth order Gaussian derivative, obtained from its Fourier transform, is

$$|X_n(f)| = (2\pi f)^n \exp\left\{-\frac{(2\pi f\sigma)^2}{2}\right\} \cdot \tag{4}$$

By differentiating (4) and setting it equal to zero, the peak transmission frequency f_p, at which the maximum is attained, can be found to satisfy the following:

$$2\pi f_p \sigma = \sqrt{n} \cdot \tag{5}$$

Then, the Gaussian derivatives of higher orders are characterized by a higher peak frequency while reducing the shape factor σ shortens the pulse. Notice that the PSD of the first order Gaussian derivative does not meet the FCC requirement no matter what value of pulse width is used. Moreover, increasing the order of the derivative results in a wider overall pulse width for each successive pulse and, consequently, in a narrower bandwidth around the same center frequency, thereby showing a better fit to the FCC masks. Indeed, as the pulse order increases, the number of zero crossings in the same pulse width also increases. The pulses then begin to resemble sinusoids modulated by a Gaussian pulse-shaped envelope, thus corresponding to a higher "carrier" frequency sinusoid modulated by an equivalent Gaussian envelope [2].

C. Underground UWB Channel Model

The considered discrete impulse response of the UWB channel model for an underground mine is expressed as follows:

$$h(t) = \sum_{l=0}^{L-1} \alpha_l \delta(t - \psi_l), \tag{6}$$

where $\delta(t)$ is the Dirac delta function, L is the number of multipath components; $\{\alpha_l\}$ and $\{\psi_l\}$ are, respectively, the gain and the delay introduced by the l^{th} path of the channel. Note that a complex tap model is not adopted here. The complex baseband model is a natural fit for narrowband systems to capture channel behavior independently of carrier frequency, but the motivation breaks down for UWB systems where a real-valued simulation at RF may be more natural [9]. As for the IEEE.802.15.3a standard model, a lognormal distribution has been used for the multipath gain. For the data measurements obtained in the considered mining environment, this chosen distribution was confirmed by the Kolmogorov-Smirnov test [10].

Furthermore, as in the Saleh-Valenzuela model the first ray starts by definition at $t=0$, and the successive rays arrive

with a rate given by a Poisson process with rate λ=1.15 $(ns)^{-1}$ (i.e. of 2.3 rays per chip). The power of these rays decays exponentially with increasing delay from the first ray. However, for the considered mining environment and in contrast to what was reported for more conventional indoor environments with smooth surfaces [9] [11], no path clustering effect was observed, neither in NB/WB measurements [12], nor in the LOS scenario at recent UWB measurements work done in such confined environments with rough surfaces [10]. Indeed, since this work is intended for a ranging application, we focus only on the LOS scenario where the first path is assumed to be the direct and strongest. Figs. 2 and 3 show, respectively, a typical underground impulse response and its corresponding lognormal PDF.

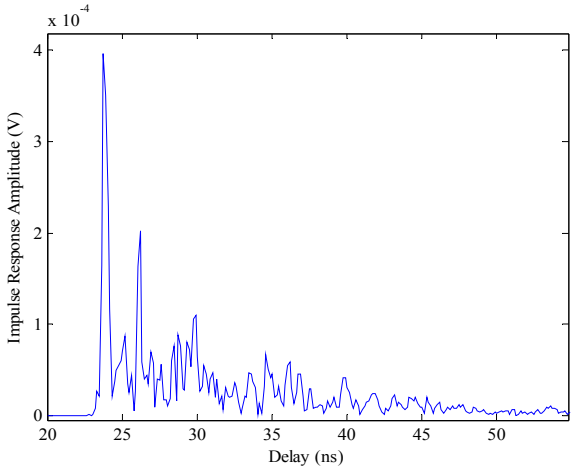

Fig. 2: Typical underground impulse response in LOS scenario.

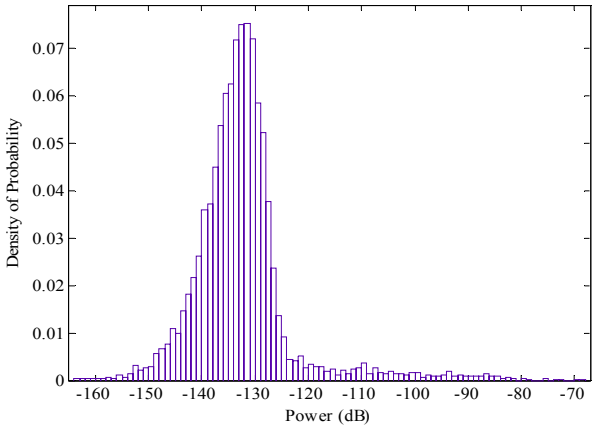

Fig. 3: Probability Density Function of the received signal in LOS scenario.

A threshold of 40 dB below the strongest path was chosen to avoid the effect of noise on the statistics of multipath channel [10]. Hence in the interest of simplicity, we consider the impulse response restricted to L=3 paths (*i.e.* two interfering paths to the direct first path). As for our ranging application we focus on the direct path (*i.e.* strongest), its gain is normalized to unity. The lognormal fading statistics of the two interfering paths are as expressed in Table I. Their relative variance is, as it seems intuitively clear, smaller for small gain than for large one, a fact that was confirmed, e.g. in [13].

TABLE I. LOGNORMAL FADING PARAMETERS

Interfering Paths	Lognormal Statistics	
	$E[\alpha_l]$	$Var[\alpha_l]$
l=1	0.5	0.09
l=2	0.25	0.04

D. UWB Receiver

When N_u users are active within the system, while focusing on the first transmitter, the signal at the receiver can be modeled as

$$r(t) = \sum_{l=0}^{2} c_l s_{pr}^{(1)}(t-\theta_l) + n_g(t), \quad (7)$$

where c_l the is the amplitude fading factor on the l^{th} path, θ_l is a summation of the delay ψ_l exclusively introduced by the l^{th} path and the phase-shift $\tau^{(k)}$ that corresponds to the TOF between the transmitter k and the considered receiver. θ_l is exponentially distributed (μ=0.87), the fading factor c_l of the interfering paths is lognormally distributed as

$$20\log_{10}(c_1) \propto N(-0.8469,\ 0.3075), \quad (8)$$

and

$$20\log_{10}(c_2) \propto N(-1.6336,\ 0.4947), \quad (9)$$

based on the values expressed in Table I, and $n_g(t)$ is

$$n_g(t) = \sum_{k=2}^{N_u}\sum_{l=0}^{2} s_{pr}^{(k)}(t-\theta_l) + n(t), \quad (10)$$

in which $s_{pr}(t)$ corresponds to $p_{pr}(t)$, the processed pulse shape at the receiver (antenna effect). $n(t)$ represents the received Gaussian noise modeled as $N(0, \sigma_n^2)$ with a power spectral density of $N_0/2$.

III. DS-UWB FAST ACQUISITION SYSTEM

For fast and accurate acquisition of UWB signals with optimal receiver complexity, the *Block-Processing* technique was used with an *FFT-based high-speed* frequency correlator. Synchronization is performed by an FFT-based circular correlator fed by the processed blocks. The block length M is taken as of power-of-two; thus the FFTs have an optimal butterfly structure. Therefore, the correlation is computed in the frequency domain by a simple

multiplication, producing the same result as the standard correlation but faster with this high-speed correlation technique. The block diagram of the considered UWB fast acquisition system is shown in Fig. 4. For a sampling rate F_s=*8* Gsps used over a spreading factor N_c=63 and a pulse duration T_p= T_c=2 ns (duty cycle of 100 %), the acquisition process is accelerated by handling the dense DS-UWB signal in simultaneous blocks of samples and by reducing the computational cost by a factor of 48 [8]. The processed DS-UWB received signal can be modeled as

$$r_{i,u}^{(j,N_u)} = d_{u,\tau_i}^{(j,k)} c_{i,\tau_i}^{(j,k)} p_{pr}\left((m_i+u) - jT_f - \frac{N_c}{M}(m_i+u)\,T_c - \tau_i^{(k)} \right) + n_{f_{(i,u)}} + n_{g_{(i,u)}}^{N_u}, \quad (11)$$

where $p_{pr}()$ represents the processed pulse shape at the receiver (antenna derivative effect), n_f is the interference signal, u refers to the u^{th} sample (u=1, 2, …, M) of the i^{th} block, m_i is the total number of samples before the i^{th} block (m_i=*(i-1).M*) and k corresponds to the acquired user at the receiver.

Since the received signal $r_{i,u}$ and the local pulse-shaped replica corresponding to the acquired MLS spreading code c_{i,τ_i} are both finite length sequences, their correlation can be carried out by a slight modification of the circular convolution operation. Indeed, the correlation of these two sequences is obtained by tacking the product of their discrete Fourier transforms DFTs while the local pulse-shaped replica is time reversed, thus a complex conjugate is applied. Therefore, the resulting correlation performed in the frequency domain, $R_{i,u}$, of the i^{th} received signal block, $r_{i,u}$, with the local pulse-shaped replica of the k^{th} user, can be expressed as the following:

$$R_{i,u}^{(k)} = IDFT\left\{ DFT\left\{ r_{i,u}^{(N_u)} \right\} \cdot DFT^{*}\left\{ c_i^{(k)} p_{pr}\left[(m_i+u)\cdot\left(1 - N_c T_c / M\right) \right] \right\} \right\}. \quad (12)$$

In practice, the FFT is used as an efficient algorithm, to calculate the DFTs required in this frequency-domain correlation operation.

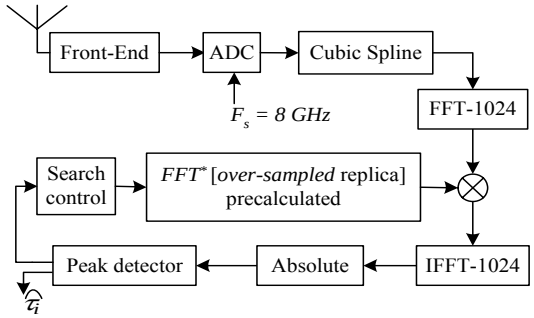

Fig.4: Block diagram of the UWB fast acquisition system.

As shown in Fig. 4, a *cubic spline interpolation* is used as an *over-sampling* method to increase the cardinality of the blocks, digitized by the ADC converter, from 1008 samples to $M=(N_c+1)\cdot T_c \cdot F_s$=1024 (*i.e.* power-of-two) in order to make possible the use of FFTs with a butterfly structure. The FFT used for the local pulse-train MLS code-replica is pre-calculated so that only one FFT/IFFT pair is used in the fast correlator structure. A peak detector examines its outputs (1024 inverse-FFT outputs) to evaluate the detected peak amplitude and to deduct its position which corresponds to the estimated phase-shift τ_i. The more blocks are acquired; the more refined will be that estimated phase which represents the TOF required for ranging with respect to the acquired user. If no peak is detected according to a detection threshold D_T, the search control block leads the local code generator index to the next pre-calculated replica *k+1*. To locate itself, the claimant (*i.e.* receiver) can use 2D-trilateration with respect to two *verifiers* (*i.e.* static transmitters).

In order to characterize the relative amplitude of the detected peak with respect to false correlations due to interferences and noise, an acquisition margin is considered. Since the direct path amplitude is normalized to unity, while the noise level is set bellow 18 %, an acquisition margin of 14.9 dB is used for the detection.

IV. Simulation Results

In this section, the performance of the UWB multiple-access fast acquisition system in the considered multipath channel scenario is evaluated by extensive Monte-Carlo simulations using 100 000 samples. The performance are assessed in terms of the obtained positioning error range which corresponds to the synchronization error obtained while estimating the phase-shift τ. The performance of the first eleven Gaussian derivatives and the doublet waveforms are compared while used within the studied UWB fast acquisition system to determine the most suitable pulse shape to consider in the multipath scenario for that proposed scheme. Moreover, the obtained performance of the studied computationally-efficient system is compared with respect to the unipath case under different levels of MUI and AWGN. The PN sequences of the interfering sources are randomly selected from N_{umax}=6 MLS codes of period N_c=63. Moreover, the users are supposed to be asynchronously in motion inside the mine gallery, thus, the corresponding phase-shifts are randomly varying within the frame of the code-period duration. Figs. 5 and 6 show the performance levels of, respectively, the simulated waveforms within the proposed fast acquisition system, and for both scenarios of multipath and unipath compared under different MUI and AWGN levels. Results suggest that the best performance score is obtained by the 3rd, 4th and 10th Gaussian derivatives. These waveforms are the most suitable pulse shapes to choose, depending on the spectral bandwidth requirements and compliance to the FCC regulations. Indeed, as the derivative order increases, the peak transmission frequency increases and the signal bandwidth decreases. Hence, choosing the most appropriate derivative order is a trade-off with the effective bandwidth for a desired performance level. For the three first order derivatives, irrespective to their performance, these pulses do not meet the FCC spectral masks [14] and cannot satisfy it, irrespective of the pulse duration. Therefore, the 4th-order Gaussian derivative has been validated for this studied UWB fast acquisition system in the considered asynchronous multiple-access indoor

channel, for simultaneously fulfilling the FCC regulated masks and offering interesting ranging capabilities while maximizing the corresponding bandwidth. For this waveform, we note a maximum gap of less than 0.6 meters in the positioning error range between the multipath and unipath scenarios. However, since we obtain for the worst case (*i.e.* maximum interfering sources within the system with a high level of noise; σ_N^2=5) a location estimation accuracy of 0.78 meters which is very acceptable for the desired ranging application, we consider the suggested fast acquisition system well-suited for such underground environment.

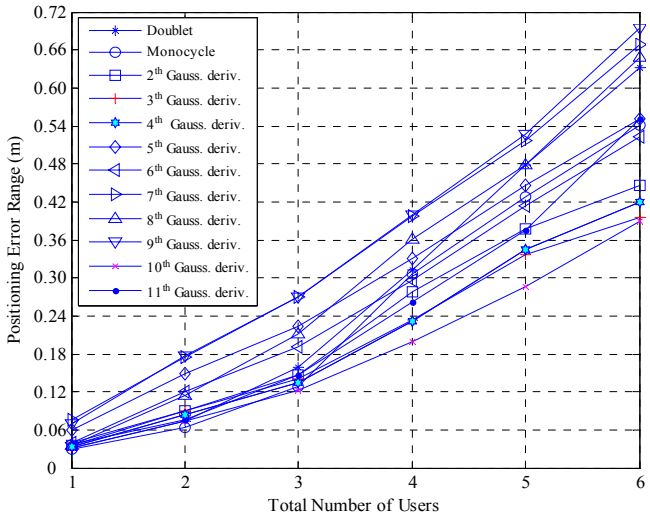

Fig.5: Pulse shapes performance comparison in multipath scenario under MUI and AWGN (σ_N^2=2).

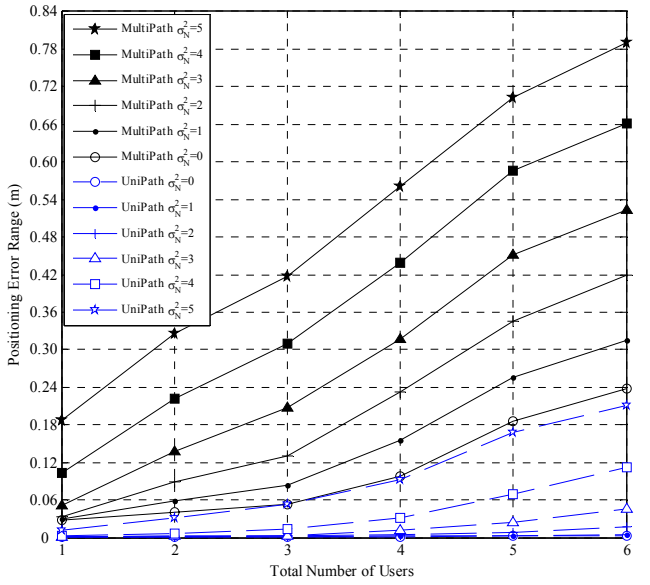

Fig. 6: Performance comparison between multipath and unipath scenarios under MUI and AWGN levels.

V. CONCLUSION

In this paper, the effect of various waveforms on the performance of a new UWB fast acquisition scheme has been evaluated in the presence of MUI and AWGN and compared in a peculiar indoor multipath fading channel. The results have shown that the pulse shape have a clear impact on the performance of the studied UWB computationally efficient acquisition system and it was concluded that the 4th-order Gaussian derivative is the most suitable waveform to adopt in this system operating in such considered underground environment. Moreover, comparisons of the suggested fast acquisition system have been made between the considered multipath fading channel and a unipath scenario, with respect to the obtained location estimation precision. The proposed system has shown very acceptable positioning error range for the considered mining confined environment.

REFERENCES

[1] Federal Communications Commission "Revision of part 15 of the commission's rules regarding ultra-wideband transmission systems," First Report and Order, ET Docket 98-153, April 2002.

[2] M. Welborn and J. McCorkle, "The importance of fractional bandwidth in ultra-wideband pulse design," *Proc. IEEE Int. Conf. Communications*, vol. 2, pp. 753-757, April 2002.

[3] H. Sheng, P. Orlik, A.M. Haimovich, L.J. Cimini, and J. Zhang, "On the spectral and power requirements for ultra-wideband transmission," *Proc. IEEE Int. Conf. Communications*, vol. 1, pp.738-742, May 2003.

[4] B. Hu and N.C. Beaulieu, "Pulse shapes for ultrawideband communication systems," *IEEE Trans. on Wireless Communications*, vol. 4, pp. 1789-1797, July 2005.

[5] M.U. Mahfuz, K.M. Ahmed, R. Ghimire and R.M.A.P. Rajatheva, "Performance comparison of pulse shapes in STDL and IEEE 802.15.3a models of the UWB channel," *Proc. IEEE ICICS'05*, pp.811-815, Dec. 2005.

[6] S.R. Aedudodla, S.Vijayakumaran and T.F.Wong, "Timing acquisition in ultra-wideband communication systems," *in IEEE Trans. on Vehicular Technology*, vol. 54, pp.1570-1583, September 2005.

[7] L. Reggiani and G. M. Maggio, "Rapid search algorithms for code acquisition in UWB impulse radio communications," *in IEEE Journal on Selected Areas in Comm.*, vol. 23, no. 5, pp. 898-908, May 2005.

[8] Y. Salih-Alj, C. Despins, and S. Affes, "A computationally efficient implementation of a UWB fast acquisition scheme," in *Proc. IEEE VTC'07-Spring*, pp. 1554-1558, April 2007.

[9] J. R. Foerster, M. Pendergrass and A. F. Molisch, "A channel model for ultrawideband indoor communication," in *Wireless Personal Multimedia Communications WPMC'03*, Vol. 2, pp. 116–120 October, 2003.

[10] Y. Rissafi, "Characterization and modeling of ulta-wideband channel in an underground mine," Masters's thesis, University of Quebec at Outaouais, Canada, June 2007.

[11] A.A. Saleh, R. A. Valenzuela, "A statistical model for indoor multipath propagation," in *IEEE Joumal on Selected Areas in Communications*, Vol. 5, No. 2, pp. 128–137, Feb. 1987.

[12] M. Boutin, A. Benzakour, C. Despins and S. Affes, "Radio wave characterization and modeling in underground mine tunnels," *in IEEE Trans. on Antennas and Propagation*, vol.: 56, pp.: 540-549 Feb. 2008.

[13] D. Cassioli, Moe Z. Win and Andreas F. Molisch, "The ultra-wide bandwidth indoor channel: from statistical model to simulations", in *IEEE Journal on Selected Areas on Communications*, Vol. 20, No. 6, pp. 1247–1257, August 2002.

[14] L.L. Zhou and H. Zhu, "Waveform design and performance analysis of ultra-wideband (UWB) pulse based on iterative algorithm," *Proc. IEEE CEEM'06*, pp. 755-758, August 2006.